Desalination and Water Treatment 321 (2025) 100941

Contents lists available at ScienceDirect

Desalination and Water Treatment

journal homepage: www.sciencedirect.com/journal/desalination-and-water-treatment/

Simultaneous nutrient-abundant hydroponic wastewater treatment, direct carbon capture, and bioenergy harvesting using microalgae–microbial fuel cells

Yustika Desti Yolanda [a], Sangsik Kim [b,c], Weonjung Sohn [d], Ho Kyong Shon [d], Euntae Yang [e,*], Sungyun Lee [a,f,**]

[a] School of Advanced Science and Technology Convergence, Kyungpook National University, 2559 Gyeongsang-daero, Sangju-si, Gyeongbuk 37224, Republic of Korea
[b] Department of Energy Chemical Engineering, Kyungpook National University, 2559 Gyeongsang-daero, Sangju-si, Gyeongbuk 37224, Republic of Korea
[c] Convergence Research Center of Mechanical and Chemical Engineering, Kyungpook National University, 2559 Gyeongsang-daero, Sangju-si, Gyeongbuk 37224, Republic of Korea
[d] School of Civil and Environmental Engineering, University of Technology, Sydney, NSW 2007, Australia
[e] Department of Marine Environmental Engineering, Gyeongsang National University, Gyeongsangnam-do 53064, Republic of Korea
[f] Department of Environmental and Safety Engineering, Kyungpook National University, 2559 Gyeongsang-daero, Sangju-si, Gyeongbuk 37224, Republic of Korea

HIGHLIGHTS

- mMFCs were explored for nutrient recovery from hydroponic wastewater and energy generation.
- The mMFCs demonstrated CO_2 fixation and algal biomass production.
- Microalgae enabled aeration-free operation, potentially reducing energy use.
- Anodic pH 6 outperformed pH 7 and 8 in MPD, COD removal, and TN removal efficiency.
- The mMFCs removed 22.6 % TAN and 100 % PO_4^{3-} in cathode chamber.

GRAPHICAL ABSTRACT

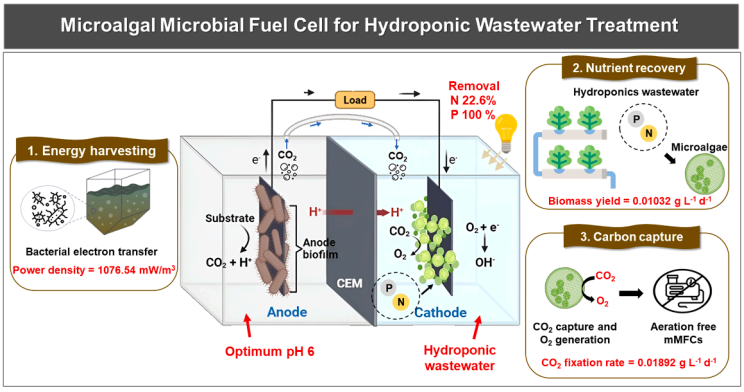

ARTICLE INFO

Keywords:
Microalgae–microbial fuel cell
Hydroponic wastewater
Nutrient removal
Energy recovery
Carbon capture

ABSTRACT

Hydroponics has increasingly been recognized as an important agricultural method due to its stable crop yields under rapidly changing environmental conditions. However, the efficient treatment of nutrient-rich hydroponic wastewater remains a major challenge. This study investigates the effect of anodic pH on the performance of microalgae–microbial fuel cells (mMFCs), focusing on bioelectricity generation, photosynthetic oxygen supply, nutrient removal and recovery, and carbon capture. The mMFC system achieved a maximum power density of 122.5 mW/m^2, a chemical oxygen demand removal efficiency of 93.7 %, and an anode-side total nitrogen

* Corresponding author.
** Corresponding author at: Department of Environmental and Safety Engineering, Kyungpook National University, 2559 Gyeongsang-daero, Sangju-si, Gyeongbuk 37224, Republic of Korea.
E-mail addresses: yet83@gnu.ac.kr (E. Yang), sungyunlee@knu.ac.kr (S. Lee).

https://doi.org/10.1016/j.dwt.2024.100941
Received 7 September 2024; Received in revised form 13 November 2024; Accepted 4 December 2024
Available online 5 December 2024

removal efficiency of 27.5 % at an acidic anodic pH. In addition, the cathode chamber had a total ammonium nitrogen removal efficiency of 22.6 %, which was ascribed to a combination of ammonium migration and subsequent nitrogen assimilation, and a phosphate removal efficiency of 100 %, likely due to microalgal uptake and adsorption. The mMFC also effectively captured CO_2 with an algal biomass yield of 0.01379 $g{\cdot}L^{-1}{\cdot}d^{-1}$ and a CO_2 fixation rate of 0.02528 $g{\cdot}L^{-1}{\cdot}d^{-1}$. These findings provide insights into the optimization of mMFCs as a sustainable solution for managing nutrient-rich hydroponic wastewater, contributing to energy-efficient and resource-recovering wastewater treatment technologies.

1. Introduction

Hydroponic systems have emerged as a viable solution to the potentially severe effect of climate change on crop production because they allow for more efficient water management and do not rely on soil or high levels of mineral fertilizers [1]. In addition, the use of nutrient solutions ensures that crop growth is precisely managed, resulting in higher productivity and more effective disease and pest management. Hydroponics also promotes resource recycling, increases environmental sustainability, and maximizes space efficiency [2]. Consequently, the demand for hydroponic agriculture has rapidly increased worldwide [3].

However, nutrient dosing in hydroponic systems often exceeds plant requirements, leading to nutrient-rich effluents. The development of effective wastewater treatment and recovery technologies for these systems remains a major challenge. Hydroponic effluents typically contain high concentrations of nitrates and phosphates, reaching up to 1000 mg/L and 200 mg/L, respectively [4]. The discharge of this nutrient-rich hydroponic wastewater can have significant environmental impacts, such as altering microbial community structures, promoting the dominance of cyanobacteria, increasing the levels of harmful cyanotoxins, and reducing biodiversity [5].

For this reason, to ensure sustainable hydroponic agriculture, it is necessary to develop water treatment systems capable of handling high nutrient loads and recovering these nutrients for reuse. These systems also need to be energy efficient and carbon neutral. However, traditional wastewater treatment processes struggle to meet these requirements because they involve energy-intensive methods that contribute to greenhouse gas emissions and generate large quantities of sludge that require disposal and management, leading to further environmental concerns [6]. In addition, most traditional treatment approaches cannot recover valuable resources present in the wastewater such as ammonia, phosphate, and metals [7]. This limitation suggests deficiencies in current approaches and indicates the need to develop innovative technologies that can address these challenges.

Microbial fuel cells (MFCs) have been developed as a potential option for sustainable wastewater treatment. These bioelectrochemical systems are versatile in that they can simultaneously treat water and harvest energy from organic waste, thus potentially achieving self-sufficient wastewater treatment systems [8]. MFCs harness microbial metabolic redox reactions to transform the chemical energy in organic compounds and waste into electrical energy. Generally, an MFC consists of an anaerobic anode chamber and an aerobic cathode chamber separated by a cation exchange membrane (CEM) [9]. In the anode chamber, electrically active bacteria on the electrode surface play a crucial role in electron generation. These electrons, along with protons, migrate to the cathode chamber where reduction reactions occur. Oxygen is commonly used as the electron acceptor in the cathode due to its availability and favorable electrochemical properties [10].

In addition, by modifying the cathodic setup, MFCs can be employed for the recovery of valuable resources, carbon capture and utilization, chemical production, and methane and hydrogen production [11]. One such modification is the use of microalgae in the cathode chamber for aeration-free electricity generation, carbon capture, and nutrient recovery. In these microalgae–MFCs (mMFCs), rather than relying on energy-intensive mechanical aeration, the microalgae growing in the cathode chamber produce and supply oxygen via photosynthesis, ensuring electricity generation and algal biomass production. In addition, during their photosynthesis and growth, the microalgae can efficiently utilize nutrients in the wastewater and fix CO_2 from the air [12]. According to a previous report, an mMFC removed more than 88.9 % of ammonia and 80.28 % of total phosphorus with a low power density of 42 mW/m^2 [13]. In other research, CO_2 fixation rates using *Chlorella vulgaris* were reported to be 0.04 g CO_2/L/d using a sequential baffled-column photobioreactor design and 0.09 g CO_2/L/d using a cylindrical photobioreactor design [14,15]. However, despite these advancements, various challenges remain when seeking to fully harness mMFCs for hydroponic wastewater treatment, particularly in optimizing operational parameters such as the anodic pH.

In this study, we aim to address this gap by investigating the effect of the anodic pH on the performance of an mMFC, focusing on bioelectricity generation, photosynthetic oxygen supply, nutrient removal and recovery efficiency, and carbon capture. This research provides insights into the optimization of mMFCs as a promising and sustainable approach for the management of nutrient-rich hydroponic wastewater. The outcomes emphasize the potential benefits of mMFCs in achieving energy-efficient and resource-recovering wastewater treatment, thus contributing to the development of sustainable agricultural practices and wastewater treatment technologies.

2. Materials and methods

2.1. Construction and operation of the mMFC

A double-chambered mMFC was constructed for use in this study, consisting of cuboid-shaped anode and cathode chambers (Fig. 1). Both chambers had a volume of 170 mL and were separated by a PTFE fabric-reinforced perfluorosulfonic acid (PFSA) GI-N417 membrane with a thickness of 0.26 mm and an effective surface area of 25 cm^2 (5.0 ×5.0 cm) as the CEM (Fuel Cell Store, USA). The CEM was pre-expanded by immersing it in 0.1 wt% NaOH for 4–12 h, followed by rinsing with deionized (DI) water to remove impurities and protonate the sulfonic acid functional groups [16]. The electrodes were constructed by attaching carbon cloth (0.5 mg/cm^2 60 % platinum, 5 × 5 cm, Fuel Cell Store, USA) and carbon felt (3.18 mm, 99.0 %, 5 × 5 cm, Thermo Fisher Scientific) to one side of each stainless-steel plate with a hole (used as a current collector) using silver paste (CANS ELCOATT P-100). The cell arrangement setup is presented in Fig. S1. Prior to use, the carbon felt electrodes were pretreated by soaking them in 1 M HCl and 1 M NaOH solutions for 24 h, followed by rinsing with DI water to remove impurities and increase conductivity [17].

A nutrient mineral buffer (NMB, pH 7) was used as the anode electrolyte. A concentrated nutrient and mineral stock solution was first prepared containing the following components in DI water: $CoCl_2{\cdot}6H_2O$ (0.25 g/L), $FeCl_2{\cdot}4H_2O$ (2 g/L), $MnCl_2{\cdot}4H_2O$ (0.05 g/L), H_3BO_3 (0.05 g/L), $CuCl_2$ (0.015 g/L), $NaMoO_4$ (0.005 g/L), $NiCl_2{\cdot}6H_2O$ (0.025 g/L), $NaSeO_4$ (0.025 g/L), $ZnCl_2$ (0.025 g/L), $NaVO_3$ (0.025 g/L), $CaCl_2$ (15 g/L), $MgCl_2{\cdot}6H_2O$ (20 g/L), and NH_4Cl (53 g/L) [18]. The final NMB solution was prepared by adding the nutrient and mineral solution stock to 1 L of phosphate buffer solution (PBS; 50 mM, pH 7) with a dilution factor of 100, with the pH adjusted using a monovalent strong base and acid. Sodium acetate was added as the substrate (1 g/L) before

introducing it to the reactor.

The cathode chamber was filled with synthetic hydroponic wastewater prepared following the Yamazaki method for tomatoes. The following nutrients were used in the mMFC system: KNO_3 (101 mg/L), $Ca(NO_3)_2{\cdot}4H_2O$ (177 mg/L), Fe.EDTA.Na (7.65 mg/L), $NH_4H_2PO_4$ (38 mg/L), $MgSO_4{\cdot}7H_2O$ (123 mg/L), H_3BO_3 (0.72 mg/L), $MnSO_4{\cdot}H_2O$ (0.41 mg/L), $ZnSO_4{\cdot}7H_2O$ (0.045 mg/L), $CuSO_4{\cdot}5H_2O$ (0.02 mg/L), and $Na_2MoO_4{\cdot}2H_2O$ (0.005 mg/L) [19]. The concentrations of these nutrients were adjusted to ensure that the concentration of NO_3^- (309.8 mg/L), TAN (11.9 mg/L), TN (108.3 mg/L), and PO_4^{3-} (63.4 mg/L) fell within the typical range observed in actual hydroponic effluent [20,21]. All chemicals were purchased from Sigma-Aldrich (USA), Samchun Chemicals (South Korea), and Daejung Chemicals & Metals Co., Ltd. (South Korea).

Anaerobic digester sludge (2.6 % dry mass) was collected from a Seobu wastewater treatment plant (Daegu, Korea) that treats domestic wastewater. This sludge was mixed with fresh anode solution at a ratio of 20 % v/v to inoculate the anode electrode with microbial catalysts. The anode chamber containing the NMB and sludge was initially purged with nitrogen gas for 20 min to reduce the dissolved oxygen (DO) levels to 3–4 mg/L. The operation of the mMFC system was initiated with an acclimation period to allow time for bacterial biofilm to form on the anode electrode. During this phase, biofilm formation was monitored based on electricity generation. Acclimation was conducted using acetate as the substrate at an external resistance of 1 kΩ for 28 days until stable electricity production had been achieved. During the inoculation stage, the cathode chamber was filled with synthetic hydroponic wastewater without microalgae.

The anode chamber was fed with NMB once stable power output parameters had been achieved. Following this, mMFC performance was evaluated under acidic (pH 6), neutral (pH 7), and alkaline (pH 8) conditions in the anode chamber, with the pH adjusted using 1 M NaOH and 1 M HCl. A silicon tube was used to connect the anode and cathode chambers to allow the diffusion of the CO_2 generated at the anaerobic anode. Both chambers were stirred using a magnetic stirrer at 150 rpm to maintain homogenous conditions. A cool white lamp (1000 LUX) was placed near the cathodic chamber. All experiments were conducted in duplicate at room temperature (25 °C).

2.2. Cultivation of the microalga *Chlorella vulgaris*

The microalga *C. vulgaris* was initially cultivated in BMB media (Cat. No. B5282, Sigma-Aldrich) and then used to inoculate (10 % v/v) a 1 L bottle containing hydroponic solution (pH 7) until reaching an optical density (OD) of approximately 2.0, measured at 680 nm using a UV–Vis spectrophotometer (UV-1900i, Shimadzu). The cultivation setup was run under laboratory-controlled conditions (illuminance 1000 lux, 24h-light, 25 °C) using an Amazon Noiseless Aerator SH-A4 connected to a small rubber tube. At the beginning of the experiments, *C. vulgaris* cells were harvested from the pre-culture via centrifugation at 2000 rpm and diluted in fresh hydroponic medium until the OD reached 0.6. This diluted microalgal suspension was then used as the catholyte for the mMFC experiments [17].

2.3. Analytical methods and calculations

2.3.1. Evaluation of mMFC performance

The voltage (V) across the external resistance (R) was continuously monitored at 10-min intervals during operation using a multimeter (2700 Data Acquisition Series, Keithley Instruments, USA). The multimeter was directly connected to the anode and cathode electrodes using copper wire. The current (I) was calculated using Ohm's law (Eq. 1):

$$I = \frac{V}{R} \tag{1}$$

After the system had stabilized, the external load was varied ranging from 500 kΩ to 10 Ω to obtain polarization and power curves [17]. An external resistance load of 500 Ω was applied as the optimal external resistance based on the polarization test (Fig. 2) [22]. The current density (I_{den}) and power density (W_{den}) were normalized to the electrode

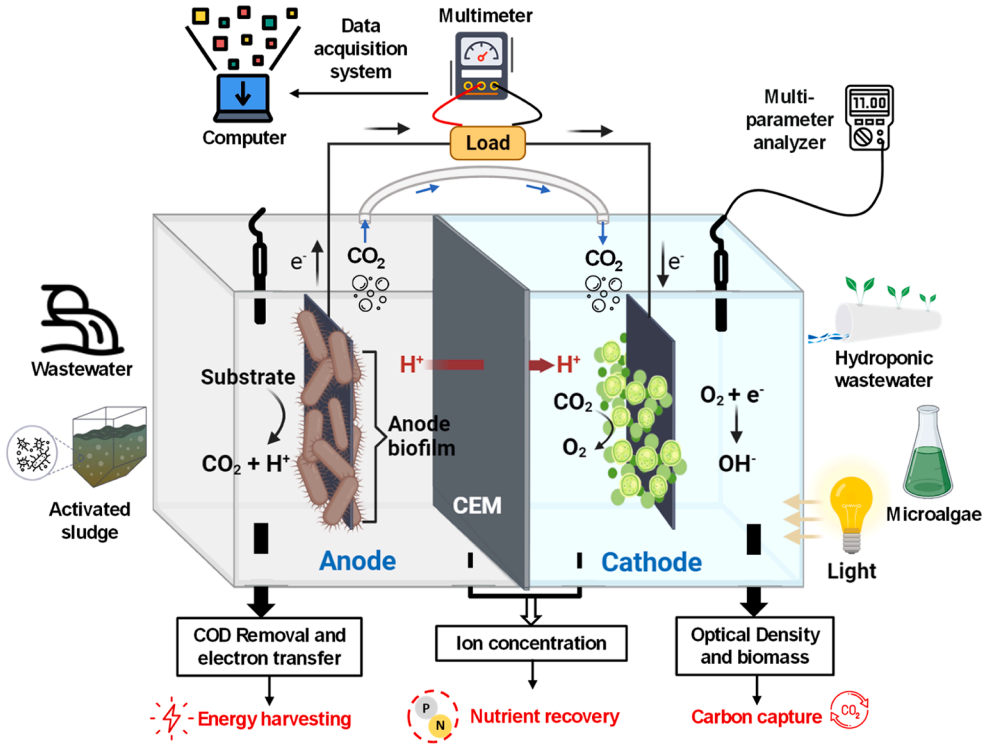

Fig. 1. Schematic diagram of the proposed mMFC used to treat hydroponic wastewater. Key outputs include electricity generation, CO_2 fixation, and nutrient recovery in the form of microalgal biomass.

surface area (A) using Eqs. (2) and (3), respectively:

$$I_{den} = \frac{I}{A} \tag{2}$$

$$W_{den} = \frac{V \times I}{A} \tag{3}$$

The Coulombic efficiency (CE) was calculated using Eq. (4):

$$CE = \frac{8 \int_0^t Idt}{FV_A \Delta COD} \tag{4}$$

where V_A is the effective anode volume, I is the current, ΔCOD is the change in the chemical oxygen demand (COD) over time t, and F is the Faraday constant (96,485 C/mol). The COD was calculated by converting the dissolved organic carbon (DOC) values using a COD/DOC ratio of 2.3, as established for acetate [23]. The COD and total nitrogen (TN) removal efficiency in the anode chamber was calculated using Eqs. (5) and (6), respectively:

$$\text{COD removal} = \frac{([COD_i] - [COD_f])}{([COD_i])} \times 100 \tag{5}$$

$$\text{TN removal} = \frac{([TN_i] - [TN_f])}{([TN_i])} \times 100 \tag{6}$$

where $[COD_i]$ and $[COD_f]$ are the initial and final COD concentrations at the anode, respectively, while $[TN_i]$ and $[TN_f]$ are the initial and final TN concentrations at the anode, respectively [24,58].

The ammonia removal rate was determined based on the total ammonia nitrogen (TAN) levels (mg/L/h) using Eq. (7):

$$\text{TAN removal rate} = \frac{\left((C_{in-an} + C_{in-cat}) - C_{eff-an}\right) \times V_{an} + \left((C_{in-an} + C_{in-cat}) - C_{eff-cat}\right) \times V_{cat}}{t} \tag{7}$$

where C_{in-an} and C_{in-cat} represent the initial TAN concentration at the anode and cathode, respectively. C_{eff-an} and $C_{eff-cat}$ are the TAN concentration in the anode and cathode effluent, respectively, V_{an} and V_{cat} are the volume of the anode and cathode chambers, respectively, and $\boldsymbol{t}$ is the experimental duration [25].

The microalgal biomass yield was measured as the average daily biomass concentration of the microalgae, which was used to monitor growth trends. The yield was calculated using Eq. (8):

$$P_m = \frac{C_{mt} - C_{m0}}{t} \tag{8}$$

where P_m is the biomass yield of microalgae ($g{\cdot}L^{-1}{\cdot}d^{-1}$), C_{m0} is the initial biomass concentration (g/L), and C_{mt} is the biomass concentration on day t [26]. The biomass concentration (g/L) was calculated using the equation $y = 0.4076\ OD_{680} - 0.0052$ ($R^2 = 0.999$) based on the calibrated optical density (OD_{680}) to biomass dry weight for *C. vulgaris* [27]. In addition, the CO_2 fixation rate ($g{\cdot}L^{-1}{\cdot}d^{-1}$) was calculated using Eq. (9):

$$CO_2 \text{ fixation rate } (g{\cdot}L^{-1}{\cdot}d^{-1}) = W_{dry} \times C \times \frac{m_{CO_2}}{m_C} \tag{9}$$

where W_{dry} is the dry biomass concentration ($g{\cdot}L^{-1}{\cdot}d^{-1}$), C is the carbon content (0.5), and m_{CO_2} *and* m_C is the molecular mass of CO_2 and C (g/mol), respectively [28].

The oxygen consumption rate ($g{\cdot}L^{-1}{\cdot}d^{-1}$) was determined by first calculating the moles of oxygen consumed according to the stoichiometry of the oxygen reduction reaction (ORR), where 4 moles of electrons reduce 1 mol of oxygen ($O_2 + 4e^- + 4H^+ \rightarrow 2H_2O$). This relationship was then used to convert the total moles of electrons to the oxygen consumption rate, as shown in Eq. (10):

$$O_2 \text{ consumption rate } (g{\cdot}L^{-1}{\cdot}d^{-1}) = \frac{2}{F \times V_{chamber}} \int_0^t I\, dt \tag{10}$$

The normalized energy recovery (NER) was used to describe the MFC energy production in kWh/m^3 and kWh/kg COD by considering the treatment capacity and the conversion of organic compounds to energy, as shown in Eq. (11) and (12) [29]:

$$NER_v (kWh/m^3) = \frac{P[KW] \times t[h]}{V[m^3]} \tag{11}$$

$$NER_{COD} (kWh/kgCOD) = \frac{P[KW] \times t[h]}{V[m^3] \times \Delta COD\ [Kg_{COD}.m^{-3}]} \tag{12}$$

2.3.2. Water quality measurements

The DO, conductivity, and pH in the anode and cathode chambers were analyzed using a HACH HQ40d-meter equipped with appropriate electrodes (Hach Company, Loveland, CO, USA). Anode samples were collected at the end of each four-day cycle, while cathode samples were collected daily. The collected samples were filtered using a microfilter syringe (0.45 μm, cellulose acetate, Chemlab, Barcelona) and stored at 4 °C until further analysis.

TN and DOC were measured using a total organic carbon analyzer coupled with a TN measuring unit (TNM-L and TOC-L, Shimadzu). UV_{254} absorbance was measured at a wavelength of 254 nm using a UV–Vis spectrophotometer (UV-1900i, Shimadzu). The concentrations of NO_3^-, NO_2^-, and PO_4^{3-} anions were determined simultaneously using ion chromatography (Dionex ICS-1100, Thermo Scientific), and ammonia concentrations were measured using the salicylate method 10031 (DR 3800 spectrophotometer, HACH).

Fluorescence excitation–emission matrix (EEM) spectra were obtained using a fluorescence spectrometer (RF-6000, Shimadzu) equipped with a 150 W Xenon lamp by collecting scans for excitation wavelengths (λ_{ex}) from 220 to 500 nm at 5 nm intervals and emission wavelengths (λ_{em}) from 250 to 550 nm at 1 nm intervals. The excitation–emission wavelength scan speed was fixed at 2000 nm/min. When conducting fluorescence excitation and emission scanning, non-fluorescent chromophores present in the sample matrix can absorb some of the light, reducing the intensity. To correct for this, the absorbance spectrum of each sample was obtained at 200–800 nm (UV-1900i spectrophotometer, Shimadzu) [30]. The population growth of *C. vulgaris* in the cathode chamber was monitored daily using the absorbance at 680 nm.

3. Results and discussion

3.1. Energy recovery performance of the mMFC

Fig. 2(a) presents the polarization power density curves for the mMFC at anolyte pH levels of 6, 7, and 8. The system exhibited the highest maximum power density (MPD) of approximately 122.5 mW/m^2 at pH 6, followed by 116.65 mW/m^2 at pH 7 and 107.2 mW/m^2 at pH 8. These results are consistent with previous studies suggesting that a slightly acidic anolyte provides an optimal growth environment for electrogenic bacteria, enhancing their electrochemical activity and

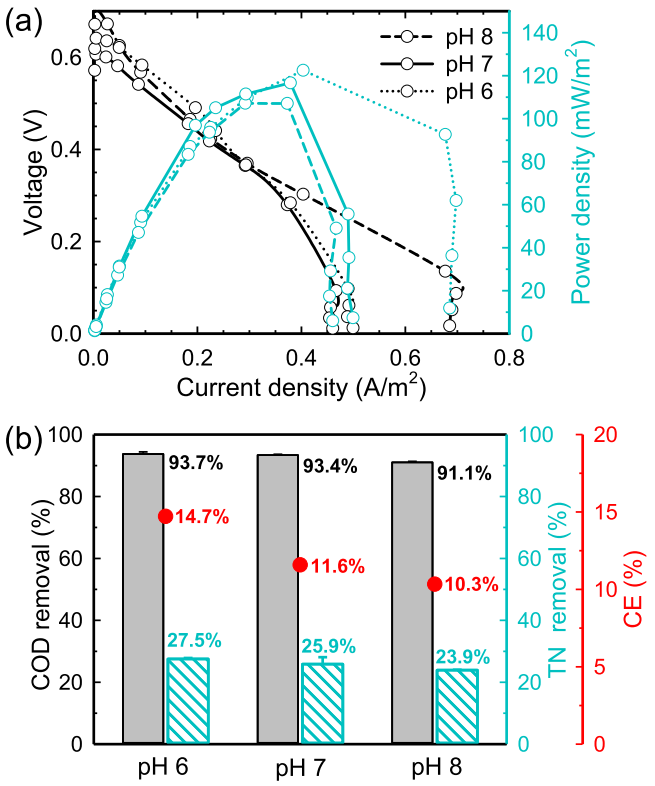

Fig. 2. (a) Polarization and power density curves and (b) COD and TN removal from the anodic chamber and the CE of the proposed mMFC with an anodic pH of 6, 7, and 8.

facilitating more efficient electron transfer [31]. For example, Reghavulu et al. observed a higher MPD under acidic conditions (65.82 mW/m^2) than at a neutral pH (49.26 mW/m^2) using ferricyanide as the catholyte [32]. Similarly, Zhang et al. reported optimal MFC performance at pH 6.5, achieving an MPD of 317 mW/m^2 [33]. Our findings suggest that the moderately acidic environment (pH 6) in the anode chamber of the mMFC enhanced the activity of the electroactive bacteria, highlighting the significance of pH control.

The addition of microalgae to the cathode chamber of MFC systems eliminates the need for an external oxygen supply because microalgae generate oxygen through photosynthesis. This advantage not only reduces operational costs but also enhances the energy production efficiency. Ullah et al. reported a microalgae-based MFC that achieved an MPD of 50 mW/m^2, which was 28 % higher than a mechanically aerated MFC [34]. This indicates that microalgae-based cathodes in MFC systems have the potential to both conserve energy and increase power generation. Our study extends this concept by adding a hydroponic solution to the cathode chamber. This novel approach aims to simultaneously remove nitrogen and phosphorus and generate electricity, distinguishing it from previous studies that have primarily focused on oxygen generation by microalgae without attempting nutrient removal.

A comparison of the performance of previously reported microalgae-based MFC systems is presented in Table 1.

Our system demonstrated a relatively high MPD, which can be attributed to the laboratory-scale nature of our experiments and the use of a carbon felt–platinum (Pt) composite as the cathode electrode. The Pt-decorated carbon felt electrode likely contributed to the greater O_2 reduction and enhanced power density observed in our study compared to systems that employ bare graphite electrodes [38,39]. It is important to note that a direct comparison between the performance of our MFC and other studies is complicated by the variation in experimental conditions. The wide range of results obtained from these MFCs also suggests that reactor size and algal species alone do not determine performance, highlighting the complex interaction between numerous factors that affect MFC efficiency.

3.2. Organic matter and nutrient removal using anodic bacteria

3.2.1. COD removal, TN removal, and CE

The COD and TN removal efficiency and CE of the proposed mMFC were assessed at different anolyte pH levels. The high COD removal rates observed for all three pH levels confirmed the successful development of mature biofilm during the setup phase before the experiments commenced [34]. As illustrated in Fig. 2(b), the mMFC with an anodic pH of 6 achieved the highest COD removal efficiency (93.7 %), followed by pH 7 (93.4 %) and pH 8 (91.1 %). This trend suggests that an anodic pH of 6 provides the most conducive environment for organic matter degradation, likely because a slightly acidic pH offers optimal metabolic conditions for electroactive bacteria [31].

However, the CE, which measures the efficiency in converting electrons generated from microbial metabolism into electricity, was consistently below 25 % for all pH levels. The maximum CE was 14.7 %, 11.6 %, and 10.3 % for anodic pH levels of 6, 7, and 8, respectively, a trend that was consistent with the COD removal efficiency. CE values consistently below 25 % indicate that electrochemical reactions play a minor role in overall COD removal [40]. This suggests that non-electrochemical processes, such as microbial respiration without electron transfer to the anode, likely involving non-electroactive bacteria species, were primarily responsible for COD removal [41].

TN removal efficiency also exhibited a similar trend, with pH 6 producing the highest removal rate with 27.5 %, compared to 25.9 % for pH 7 % and 23.9 % for pH 8 (Fig. 2a). While the mechanisms responsible for TN removal in MFCs are complex, it is generally understood that, in a closed MFC system, TN removal from the anode chamber is primarily driven by the migration of ammonium to maintain charge neutrality and diffusion due to concentration gradients, facilitating ammonium transfer from the anodic to the cathodic chamber [42]. This process is believed to have contributed to the overall TN removal in our study.

The improved COD removal, CE, and TN removal performance at pH 6 illustrates the interconnectedness of these processes. However, the consistently low CE values for all pH levels suggest that further optimization of the mMFC operational parameters is necessary to improve the CE of organic substrate removal.

3.2.2. TAN removal

The removal efficiency of TAN in the form of ammonium (NH_4^+) and

Table 1
Performance comparison of algae-based cathode MFC systems.

MFC type	Separator	Functional algae species	MPD (mW/m^2)	Anode volume (L)	COD removal	CE (%)	Ref.
Two chambers	CEM	*Chlorella vulgaris*	8.79	0.4	84.80 %	9.40 %	[35]
Two chambers	PEM	*Chlorococcum sp.* and *Synechococus sp.*	30.2 and 41.5	0.25	69.4 % and 73.5 %	16.5 % and 11.4 %	[36]
Two chambers	Salt bridge	*Spirulina platensis*	11.25	0.2	31.8	N/A[a]	[17]
Two chambers	PEM	*Scenedesmus sp.*	47.6	1	83.30 %	1.10 %	[34]
Two chambers	CEM	*Scenedesmus sp.*	81.6	1	93 %	N/A[a]	[37]
Two chambers	**CEM**	***Chlorella vulgaris***	**122.5**	**0.17**	**93.70 %**	**14.70 %**	**This study**

[a] N/A = not available

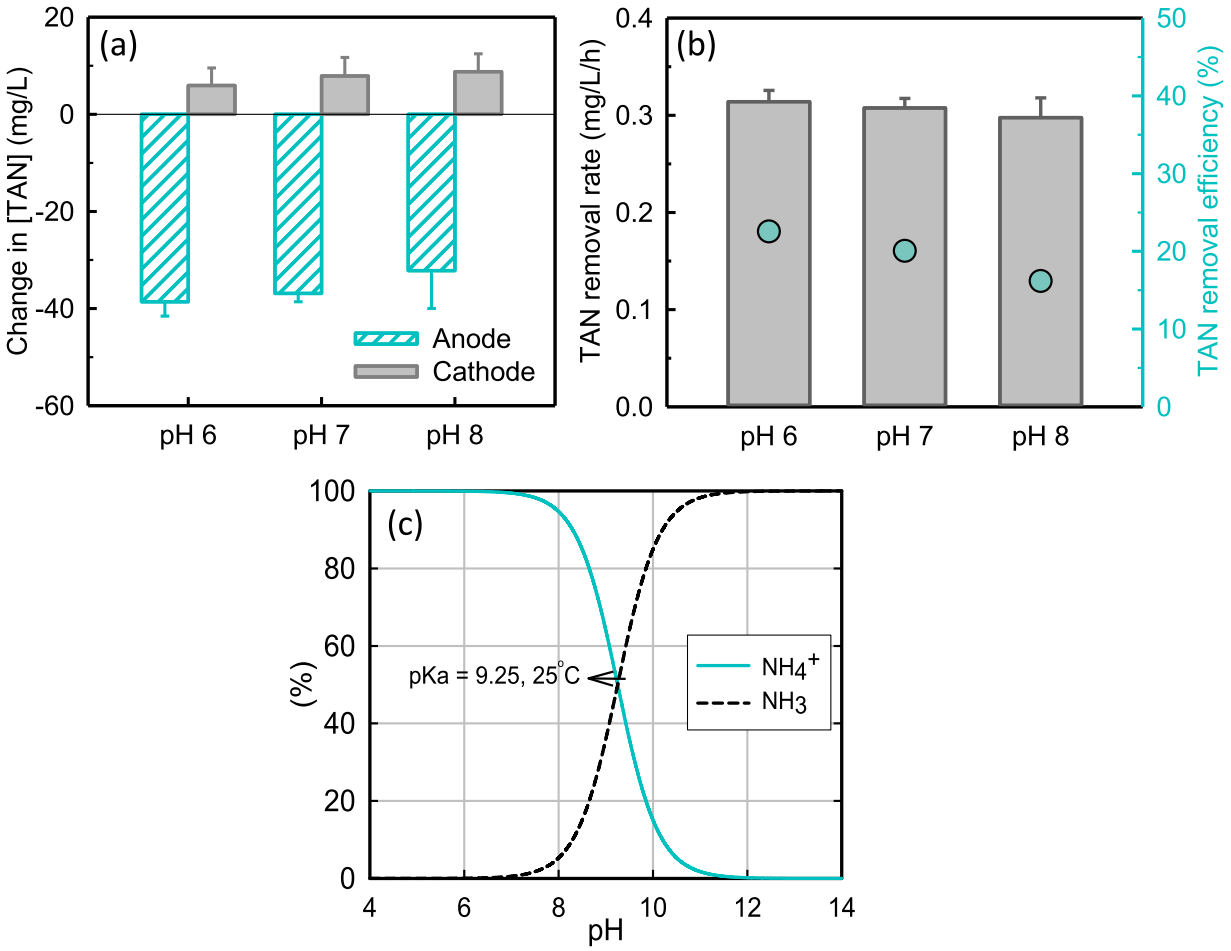

Fig. 3. (a) Concentration profile of TAN as a function of the anodic pH for the anode and cathode, (b) TAN removal rate and TAN removal efficiency of the anode as a function of the anodic pH, and (c) the partition between ammonium (NH_4^+) and ammonia (NH_3) as a function of the pH.

ammonia (NH_3) was evaluated for the mMFC system. As shown in Fig. 3 (a), the TAN concentration profiles in the anodic and cathodic chambers were monitored at different pH levels. From an initial concentration of 138.7 mg/L, TAN removal in the anodic chamber was highest at pH 6 (38.6 mg/L), followed by pH 7 (36.9 mg/L) and pH 8 (32.2 mg/L). Concurrently, the TAN concentration increased in the cathodic chamber, with the lowest increase observed at pH 6 (5.9 mg/L), followed by pH 7 (7.9 mg/L) and pH 8 (8.8 mg/L).

TAN removal rates of 0.322 ± 0.01, 0.314 ± 0.01, and 0.312 ± 0.02 mg/L/h were measured for the mMFC system at an anodic pH of 6, 7, and 8, respectively (Fig. 3b). These results are comparable to those reported by Choi et al. (2013), who observed a maximum TAN removal rate of 0.224 mg/L/h in a photobioreactor system using *C. vulgaris* [43]. The present study also recorded a TAN removal efficiency of 22.6 %, 20 %, and 16.2 % for an anodic pH of 6, 7, and 8, respectively. Notably, the mMFC system demonstrated both the highest power density (122.5 mW/m^2) and the most efficient TAN removal at pH 6. This suggests that the enhanced electricity generation at pH 6 likely contributed to more effective NH_4^+ ion migration, resulting in superior TAN removal efficiency compared to pH 7 and pH 8 levels. These results suggest that variation in the anodic pH had a minimal impact on TAN removal in the cathode chamber.

TAN removal in mMFCs is primarily driven by ammonium migration across the CEM to the cathode, a process that is facilitated by the electron flow resulting from organic substrate degradation. This electron flow promotes the transport of positively charged cations (including NH_4^+) across the CEM to maintain the charge balance, a process known as electromigration. The efficiency of TAN removal is closely associated with the current density, with a higher current density typically enhancing NH_4^+ ion migration rather than diffusion [44].

The observed pH-dependent TAN removal efficiency can also be attributed to the partitioning of TAN between NH_4^+ and NH_3, as illustrated in Fig. 3(c). The NH_4^+/NH_3 equilibrium ($NH_4^+ + OH^- \rightleftharpoons NH_3 + H_2O$) has a pKa of 9.25 at 25 °C [45]. As shown in Fig. S3(b), the anolyte was more acidic while the catholyte was basic during operation. This difference in the pH could result in a higher NH_4^+ concentration in the anolyte compared to the catholyte, potentially creating a strong diffusion flux of NH_4^+ ions [44]. Overall, the interaction between pH, microbial activity, and electrochemical processes collectively contributes to the observed TAN removal efficiencies at different pH levels in the mMFC system.

3.3. Nutrient removal by cathodic microalgae

3.3.1. Water quality parameters in the catholyte

The concentrations of DOC, PO_4^{3-}, NO_2^-, and NO_3^- in the cathode chamber were also measured as important water parameters. Fig. 4(a) shows that the initial DOC concentration in the catholyte (2.74 mg/L) increased to 8.1 mg/L at pH 6, 8.6 mg/L at pH 7, and 10.5 mg/L at pH 8 by the end of the cycle. These results could be attributed to the extracellular organic matter (EOM) produced by microalgae, which consists of various organic compounds, including carbohydrates, proteins, amino acids, lipids, and organic acids, that can increase COD/DOC levels [46]. Jiang et al. (2021) observed a similar increase in the DOC during *C. vulgaris* cultivation [47].

Fig. 4(b) shows that the phosphate concentration decreased

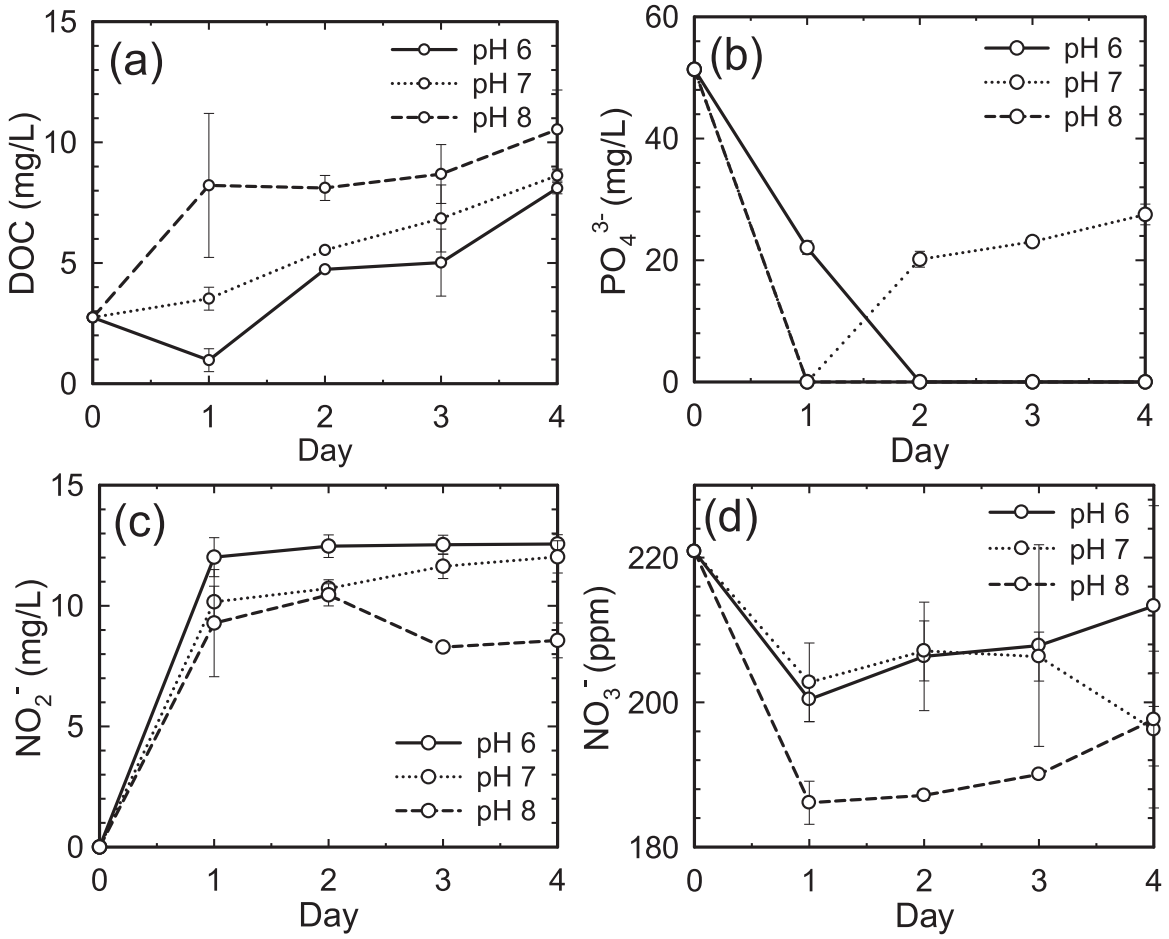

Fig. 4. Concentration of (a) DOC, (b) PO_4^{3-}, (c) NO_2^-, and (d) NO_3^- (mg/L).

significantly from an initial 51.35 mg/L to levels below the detection limit of 0.0045 mg/L at anolyte pH levels of 6 and 8 and to 23.67 mg/L at pH 7. This near-complete removal at pH 6 and 8 could be attributed to increased algal uptake via starvation and storage processes [48]. However, at pH 7, the phosphate concentration gradually increased from below the detection limit to 23.67 mg/L over three days. This was possibly due to the release of organic phosphorus or the production of soluble reactive phosphorus from decomposing algae [13].

The nitrite (NO_2^-) concentration increased over the four-day experiment, reaching 12.6 mg/L, 12.0 mg/L, and 8.6 mg/L at pH levels of 6, 7, and 8, respectively. In contrast, the nitrate (NO_3^-) concentration, which was initially 220.8 mg/L, had a negative correlation with the NO_2^- concentration (Fig. 5(d)), with removal rates of 3.4 % at pH 6, 11.1 % at pH 7 %, and 10.5 % at pH 8. This suggests that microalgae such as *C. vulgaris* assimilate nitrate as a nitrogen source for growth [45]. A pH of 6 led to the highest ammonium diffusion and removal efficiency in the anodic chamber, coupled with the lowest nitrate removal and highest increase in nitrite levels in the cathodic chamber. This can be explained by the preference of algae for assimilating ammonium over nitrate or nitrite because nitrogen must be in ammonium form for incorporation into amino acids [49].

EEM fluorescence spectroscopy was used to investigate the composition of the dissolved organic matter (DOM) in the mMFC. This method has proven to be valuable for monitoring DOM in mMFC systems. Changes in DOM were determined by analyzing the fluorescence intensities of the key peaks B, T, A, M, and C presented in Table S2. Fig. 5 reveals three main peaks: Peak B, correlated with aromatic proteins (tyrosine-like substances); Peak T, associated with soluble microbial byproducts (primarily tryptophan and protein-like substances); and Peak M, linked to marine-microbial humic-like materials [42].

Peaks B and T were highest at pH 8 (0.663 RU and 0.932 RU, respectively), followed by pH 7 (0.559 RU and 0.727 RU) and pH 6 (0.376 RU and 0.635 RU), which was in accordance with the OD measurements for the microalgae (0.5286 for pH 8, 0.5172 for pH 7, and 0.5013 for pH 6; Fig. S3d). This suggests that proteins containing tyrosine and tryptophan were produced in proportion to the biomass. Consequently, the pH 8 anodic sample, with the highest OD, also had the highest concentration of these protein-like substances, followed by pH 7 and pH 6. Conversely, Peak M, which reflects microbial activity, exhibited a different trend, with the highest intensity at pH 6 (0.497 RU) (Table S3 and Fig. S4). This demonstrates that fluorescence EEM spectroscopy is a useful tool for monitoring microalgal populations and understanding microbial dynamics in MFCs under different pH conditions.

3.3.2. *Removal mechanisms for ammonium and phosphate*

Fig. 6 shows that NH_4^+ ions transported into the catholyte were converted into NH_3 molecules due to the basic nature of the catholyte resulting from OH^- ion production [44]. The pH 6 system exhibited the highest NH_4^+ diffusion from the anode to the cathode and the highest NO_2^- formation (12.57 mg/L) compared to pH 7 (12.03 mg/L) and pH 8 (8.57 mg/L). These results are in accordance with previously reported findings that most NH_4^+-N removal can be attributed to algal assimilation [42].

Microalgae primarily assimilate inorganic nitrogen as ammonium, avoiding the energy consumption required for the reduction of nitrate to nitrite to ammonium before incorporating it into amino acids and cellular components. In particular, nitrate assimilation is initiated by the

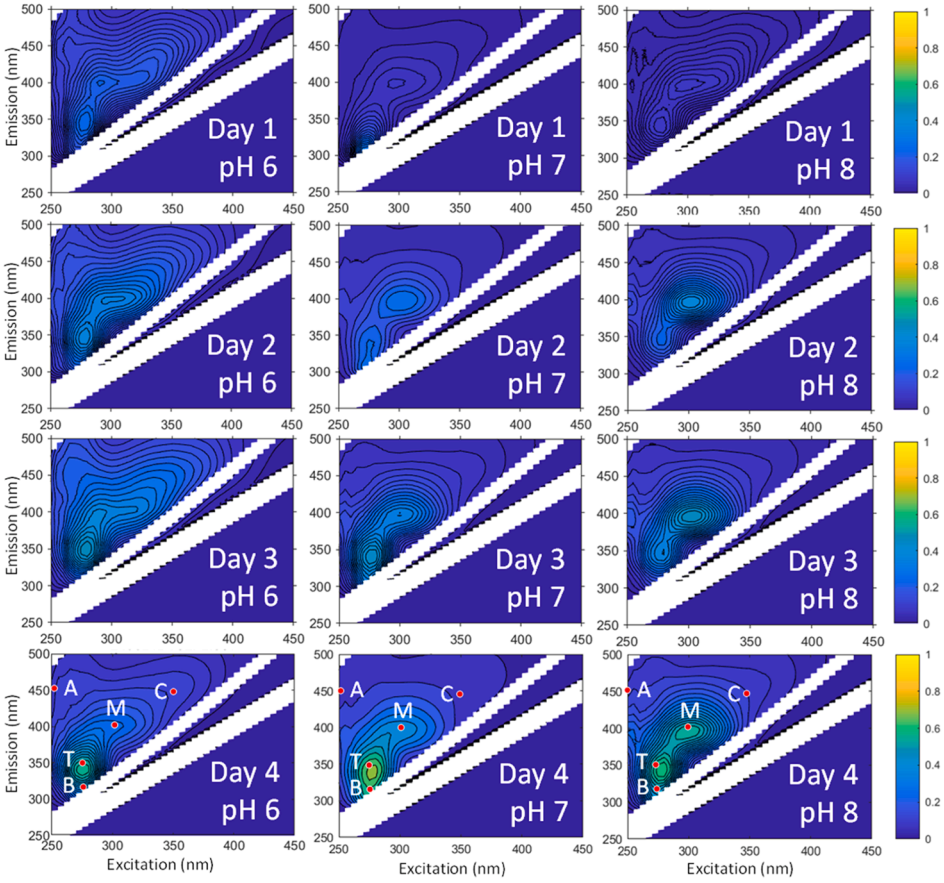

Fig. 5. Fluorescence EEMs for the catholyte during organic degradation with an anodic pH of 6, 7, and 8.

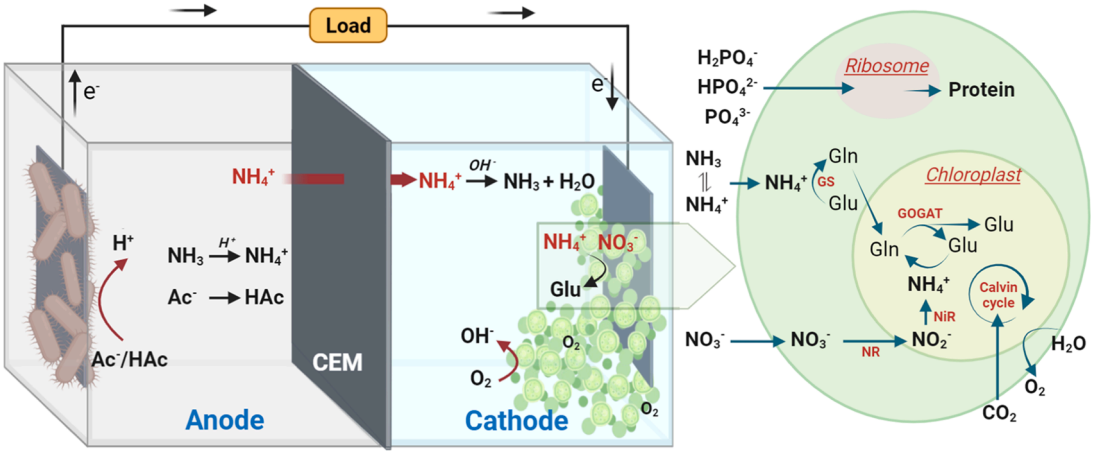

Fig. 6. Simplified schematic diagram of nitrogen migration within the mMFC system with ammonium and nitrate assimilation by microalgae. NR: nitrate reductase; NiR: nitrite reductase; GS: glutamine synthetase; GOGAT: glutamate synthase; Glu: glutamic acid; Gln: glutamine.

enzymes nitrate reductase (NR) and nitrite reductase (NiR) [50], while ammonium is directly assimilated into amino acids through the GS-GOGAT cycle, using the enzymes glutamine synthetase (GS) and glutamate synthase (GOGAT) (Fig. 6) [45]. This explains the preferential assimilation of ammonium over nitrate in *C. vulgaris*, especially when ammonium is dominant. This is in agreement with the results reported by Elmaadawy et al. (2020), who found that the nitrate concentration decreased sharply after 48 h and remained relatively constant thereafter that utilized *C. vulgaris* strain in cathode chamber [51].

When microalgae grow in an MFC cathode chamber, they absorb dissolved inorganic phosphate (PO_4^{3-}) from the environment. Phosphorus is essential for microalgae cellular functions, including energy transfer (e.g., ATP), nucleic acid synthesis (i.e., DNA and RNA), and phospholipid formation in cell membranes. Microalgae can also store excess phosphorus as acid-insoluble polyphosphate granules within their cells [52].

3.4. Carbon capture via the microalgal cathode

The carbon capture ability of the microalgal cathode in the mMFC

Table 2
Summary of the biomass yield, CO_2 fixation rate, moles of O_2 consumed, and power density for the mMFC with an anodic pH of 6, 7, and 8.

Parameters	Anodic pH		
	pH 6	pH 7	pH 8
Biomass yield ($g.L^{-1}.d^{-1}$)	0.01032 ± 0.003	0.00991 ± 0.003	0.01379 ± 0.01
CO_2 fixation rate ($g.L^{-1}.d^{-1}$)	0.01892 ± 0.006	0.01818 ± 0.006	0.02528 ± 0.02
O_2 consumption rate ($g.L^{-1}.d^{-1}$)	6.44×10^{-6}	5.05×10^{-6}	4.39×10^{-6}
Power density (mW/m^3)	1076.54	919.72	949.56

system was evaluated and the results are presented in Table 2. Microalgae in mMFCs can absorb both gaseous and soluble CO_2, enhancing their growth and productivity [53]. The highest microalgal biomass (0.01379 ± 0.01 $g{\cdot}L^{-1}{\cdot}d^{-1}$) and CO_2 fixation rate (0.02528 ± 0.02 $g{\cdot}L^{-1}{\cdot}d^{-1}$) were observed at an anodic pH of 8. The CO_2 fixation rate observed in this study was lower than that reported in previous studies focusing solely on microalgal photobioreactors (PBRs) that did not integrate MFCs. For example, Zhao et al. achieved a fixation rate of 0.09 $g{\cdot}L^{-1}{\cdot}d^{-1}$ in a fractal tree-like PBR system, while Lam and Lee reported a fixation rate of 0.04 $g{\cdot}L^{-1}{\cdot}d^{-1}$ in a sequential baffled-column PBR [14,54].

The MFC with an anodic pH of 8 also exhibited a more rapid increase in biomass compared with the anolyte at pH 7 and 6, as evidenced by the OD and biomass yield (Table 2 and Fig. S3d), but it had a lower oxygen consumption (4.39×10^{-6} $g{\cdot}L^{-1}{\cdot}d^{-1}$) and lower energy production. This could be due to self-shading within the microalgal culture, potentially reducing photosynthesis efficiency, thus decreasing the production of oxygen, which is crucial as the terminal electron acceptor in mMFCs [55]. In addition, the cathode reaction typically consumes protons during the ORR. High electricity production accelerates the ORR, consuming more protons and increasing the pH of the cathode chamber. This elevated pH can create unfavorable conditions for microalgal growth, reducing the overall CO_2 fixation ability of the system [26].

3.5. NER of the mMFC

To evaluate the feasibility of the proposed mMFC system, we used the net energy recovery (NER), a metric similar to the maximum power density (MPD) commonly reported in MFC studies, to assess the system's electricity generation performance [29]. The NER quantifies the energy value derived from the treated waste, normalized either to the reactor volume (NER_v) in kWh/m^3 or to the COD (NER_{COD}) in kWh/kg COD.

The result shows that the NER_v was 0.1033, 0.0883, and 0.0912 kWh/m^3 at a pH of 6, 7, and 8, respectively, while NER_{COD} was 0.6562, 0.5626, and 0.5958 kWh/kg COD, respectively. These results are higher than conventional and anaerobic MFC treatment processes, which generate an NER of approximately 0.057 kWh/kg COD [56]. Moreover, a study by Walter et al. (2022) reported a higher NER_{COD} of 2.092 kWh/kg COD and an NER_v of 0.335 kWh/m^3, while typical MFC systems generate an NER_v between 0.0049 and 0.1196 kWh/m^3 [57].

The enhanced performance of our mMFC system, compared with the energy production of typical MFC systems, can be attributed to the synergistic relationship between microalgae and activated sludge. This highlights the potential of integrating microalgae with activated sludge in mMFCs to enhance energy recovery and overall system efficiency. However, to fully understand the energy efficiency of the system, future studies should include energy consumption measurements that consider factors such as pumping, light illumination, and stirring requirements [56].

3.6. Economic feasibility and challenges: Recommendation for future work

The economic feasibility of scaling up mMFC technology depends on optimizing operational costs while maximizing potential outcomes. While initial investment in materials such as electrodes, membranes, and reactor components can be considerable, and methods need to be found to lower this cost where possible, reducing the need for mechanical aeration offers significant cost savings in the long term, improving the overall economic feasibility. Furthermore, the system's capacity for energy generation, nutrient recovery, CO_2 fixation, and algal biomass production increases its overall economic potential.

This study added microalgae to the cathode chamber to supply oxygen through photosynthesis, which eliminated the need for external aeration, reduced operational costs, and enhanced energy efficiency. However, despite these advantages, challenges remain for larger-scale applications, such as ensuring stable microalgae growth, managing biofilm formation, preventing electrode and membrane fouling, and maintaining stable environmental conditions (e.g., pH, temperature, and light penetration) through an integrated automated control system, which is essential for the development of effective real-world applications.

To address these issues, future studies should conduct comprehensive energy consumption analyses to complement energy production assessments. This would enable a more accurate calculation of the net energy production and provide a clearer understanding of the system's economic performance. Additionally, optimizing process parameters at the laboratory scale, such as the anodic pH, membrane configuration, microalgae type, and anolyte concentration is necessary in order to promote the development of more innovative mMFC designs and applications. In this respect, employing a full factorial design could be a valuable approach for systematically investigating the effects of these variables on system performance and scalability [58].

4. Conclusion

The present study explored the potential of mMFCs for treating nutrient-rich hydroponic wastewater. Our mMFC system added microalgae to the cathodic chamber, which provided oxygen through photosynthesis, enabling aeration-free bioelectricity generation and nutrient removal. At an optimal anodic pH of 6, the system achieved an MPD of 122.5 mW/m^2, a COD removal efficiency of 93.7 %, and an anode-side TN removal efficiency of 27.5 %. In the cathodic chamber, we observed a TAN removal efficiency of 22.6 % and complete removal of PO_4^{3-}. Collectively, these results indicate that mMFCs have the potential to effectively manage nutrient-rich hydroponic wastewater. The system also had a CO_2 fixation rate of 0.02528 $g{\cdot}L^{-1}{\cdot}d^{-1}$ and an algal biomass yield of 0.01379 $g{\cdot}L^{-1}{\cdot}d^{-1}$, showcasing its utility for carbon capture and the production of valuable by-product resources, such as feedstock for biofuel production.

The use of mMFCs in hydroponic wastewater treatment can promote sustainability, a circular economy, effective resource management, energy savings, and carbon neutrality. However, scaling up this technology requires limitations associated with system stability and economic feasibility to be resolved. While eliminating mechanical aeration reduces costs, future research should include detailed energy consumption analyses and process optimization to achieve true economic viability. Optimization efforts should focus on parameters such as the anodic pH, membrane configuration, and microalgae type, alongside advanced experimental approaches such as full factorial design. These steps will be crucial for the development of practical, scalable solutions for sustainable wastewater treatment with mMFCs, thus contributing to long-term environmental and resource management goals.

CRediT authorship contribution statement

Yustika Desti Yolanda: Writing – original draft, Visualization, Methodology, Investigation, Formal analysis. **Sangsik Kim:** Software, Methodology, Formal analysis. **Weonjung Sohn:** Writing – review & editing, Methodology. **Ho Kyong Shon:** Writing – review & editing, Conceptualization. **Euntae Yang:** Writing – review & editing, Conceptualization. **Sungyun Lee:** Writing – review & editing, Visualization, Supervision, Resources, Methodology, Conceptualization.

Declaration of Competing Interest

The authors declare that they have no known competing financial interests or personal relationships that could have appeared to influence the work reported in this paper.

Acknowledgements

This research was supported by Kyungpook National University Research Fund, 2024.

Appendix A. Supporting information

Supplementary data associated with this article can be found in the online version at doi:10.1016/j.dwt.2024.100941.

Data Availability

Data will be made available on request.

References

[1] Pomoni DI, Koukou MK, Vrachopoulos MG, Vasiliadis L. A review of hydroponics and conventional agriculture based on energy and water consumption, environmental impact, and land use. Energies 2023;16:1690.
[2] Haddad M, Abahri A. Nutrient uptake and its distribution in faba beans grown in a hydroponic system influenced by nutrients and salinity treatment. Desalin Water Treat 2022;275:233–44.
[3] Hofmann AH, Liesegang SL, Keuter V, Eticha D, Steinmetz H, Katayama VT. Nutrient recovery from wastewater for hydroponic systems: A comparative analysis of fertilizer demand, recovery products, and supply potential of WWTPs. J Environ Manag 2024;352:119960.
[4] Salazar J, Valev D, Näkkilä J, Tyystjärvi E, Sirin S, Allahverdiyeva Y. Nutrient removal from hydroponic effluent by Nordic microalgae: From screening to a greenhouse photobioreactor operation. Algal Res 2021;55:102247.
[5] Eland LE, Davenport RJ, Santos ABd, Mota Filho CR. Molecular evaluation of microalgal communities in full-scale waste stabilisation ponds. Environ Technol 2019;40:1969–76.
[6] Du R, Li C, Liu Q, Fan J, Peng Y. A review of enhanced municipal wastewater treatment through energy savings and carbon recovery to reduce discharge and CO_2 footprint. Bioresour Technol 2022;364:128135.
[7] Karimi Estahbanati MR, Kumar S, Khajvand M, Drogui P, Tyagi RD. Environmental Impacts of Recovery of Resources From Industrial Wastewater. In: Pandey A, Tyagi RD, Varjani S, editors. Biomass, Biofuels, Biochemicals, 5. Elsevier; 2021. p. 121–62.
[8] Yang E, Chae K-J, Choi M-J, He Z, Kim IS. Critical review of bioelectrochemical systems integrated with membrane-based technologies for desalination, energy self-sufficiency, and high-efficiency water and wastewater treatment. Desalination 2019;452:40–67.
[9] Hou L-g, Sun Q, Pan Z-w, Sun Z-t, Li J. Enhanced denitrification efficiency with immobilized bacteria in microbial fuel cell. Desalin Water Treat 2023;304:162–8.
[10] El-Seddik MM, Elawwad A. An extended bio-electrochemical model for wastewater treatment and water desalination: Insights into the performance of microbial desalination cells. Desalination 2024;586:117791.
[11] Sharma A, Sarkar P, Chhabra M, Kumar A, Kumar A, Kothadia H, et al. Carbon capture from petrol-engine flue gas: reviving algae-based sequestration with integrated microbial fuel cells. Chem Eng J 2023;476:146578.
[12] Salazar J, Santana-Sánchez A, Näkkilä J, Sirin S, Allahverdiyeva Y. Complete N and P removal from hydroponic greenhouse wastewater by Tetradesmus obliquus: a strategy for algal bioremediation and cultivation in Nordic countries. Algal Res 2023;70:102988.
[13] Nguyen HTH, Kakarla R, Min B. Algae cathode microbial fuel cells for electricity generation and nutrient removal from landfill leachate wastewater. Int J Hydrog Energy 2017;42:29433–42.
[14] Lam MK, Lee KT. Cultivation of Chlorella vulgaris in a pilot-scale sequential-baffled column photobioreactor for biomass and biodiesel production. Energy Convers Manag 2014;88:399–410.
[15] Sivasangari S, Vel Rajan T, Nandhini J. Aspects of photobioreactor and algadisk in CO_2 sequestration and biomass production. Energy Sources Part A Recov Util Environ Eff 2023;45:7453–60.
[16] Bazdar E, Roshandel R, Yaghmaei S, Mardanpour MM. The effect of different light intensities and light/dark regimes on the performance of photosynthetic microalgae microbial fuel cell. Bioresour Technol 2018;261:350–60.
[17] Hadiyanto H, Christwardana M, Pratiwi WZ, Purwanto P, Sudarno S, Haryani K, et al. Response surface optimization of microalgae microbial fuel cell (MMFC) enhanced by yeast immobilization for bioelectricity production. Chemosphere 2022;287:132275.
[18] Chae KJ, Choi M, Ajayi FF, Park W, Chang IS, Kim IS. Mass transport through a proton exchange membrane (Nafion) in microbial fuel cells. Energy Fuels 2008;22:169–76.
[19] Lee S, Kim YC. Water treatment for closed hydroponic systems. J Korean Soc Environ Eng 2019;41:501–13.
[20] Son J. Evaluation of the characteristics of pollutant discharge in tomato hydroponic wastewater (HWW) for sustainable water management in Korea. Water 2024.
[21] Tiwari H, Prajapati SK. Photosynthetic bioconversion of hydroponic effluent into biochemical-rich biomass for microalgal biorefineries. Environ Sci Water Res Technol 2023;9:2692–705.
[22] Aelterman P, Rabaey K, Pham H, Boon N, Verstraete W. Continuous electricity generation at high voltages and currents using stacked microbial fuel cells. Environ Sci Technol 2006;40:3388–94.
[23] Iannacone F, Di Capua F, Granata F, Gargano R, Esposito G. Shortcut nitrification-denitrification and biological phosphorus removal in acetate- and ethanol-fed moving bed biofilm reactors under microaerobic/aerobic conditions. Bioresour Technol 2021;330:124958.
[24] Shokri A, Fard MS. Kinetic, statistical, and cost evaluations in the remediation of spent caustic wastewater by photo-electro-Fenton process. Int J Environ Sci Technol 2023;20:11207–18.
[25] Zhang H, Yan Q, An Z, Wen Z. A revolving algae biofilm based photosynthetic microbial fuel cell for simultaneous energy recovery, pollutants removal, and algae production. Front Microbiol 2022;13.
[26] Yang Y-W, Li M-J, Hung T-C. The study on coupled CO_2 fixation and power generation in microalgae-microbial fuel cells embedded with oxygen-consuming biofilms. Fuel 2024;367:131410.
[27] A. Lavrinovičs, F. Murby, E. Zīverte, L. Mežule, T. Juhna, Increasing Phosphorus Uptake Efficiency by Phosphorus-Starved Microalgae for Municipal Wastewater Post-Treatment, in: Microorganisms, 2021.
[28] Lim YA, Chong MN, Foo SC, Ilankoon IMSK. Analysis of direct and indirect quantification methods of CO_2 fixation via microalgae cultivation in photobioreactors: a critical review. Renew Sustain Energy Rev 2021;137:110579.
[29] Jenani R, Karishmaa S, Babu Ponnusami A, Senthil Kumar P, Rangasamy G. A recent development of low-cost membranes for microbial fuel cell applications. Desalin Water Treat 2024;320:100698.
[30] Nurhayati M, You Y, Park J, Lee BJ, Kang HG, Lee S. Artificial neural network implementation for dissolved organic carbon quantification using fluorescence intensity as a predictor in wastewater treatment plants. Chemosphere 2023;335:139032.
[31] Garbini G, Barra Caracciolo A, Grenni P. Electroactive bacteria in natural ecosystems and their applications in microbial fuel cells for bioremediation: a review. Microorganisms 2023;11:1255.
[32] Raghavulu SV, Mohan SV, Goud RK, Sarma PN. Effect of anodic pH microenvironment on microbial fuel cell (MFC) performance in concurrence with aerated and ferricyanide catholytes. Electrochem Commun 2009;11:371–5.
[33] Zhang L, Li C, Ding L, Xu K, Ren H. Influences of initial pH on performance and anodic microbes of fed-batch microbial fuel cells. J Chem Technol Biotechnol 2011;86:1226–32.
[34] Ullah Z, Sheikh Z, Zaman WQ, Zeeshan M, Miran W, Li J, et al. Performance comparison of a photosynthetic and mechanically aerated microbial fuel cell for wastewater treatment and bioenergy generation using different anolytes. J Water Process Eng 2023;56:104358.
[35] Zhou M, He H, Jin T, Wang H. Power generation enhancement in novel microbial carbon capture cells with immobilized Chlorella vulgaris. J Power Sources 2012;214:216–9.
[36] Naina Mohamed S, Ajit Hiraman P, Muthukumar K, Jayabalan T. Bioelectricity production from kitchen wastewater using microbial fuel cell with photosynthetic algal cathode. Bioresour Technol 2020;295:122226.
[37] Ullah Z. Zeshan, Effect of catholyte on performance of photosynthetic microbial fuel cell for wastewater treatment and energy recovery. Renew Energy 2024;221:119810.
[38] Kosimaningrum W, Ouis M, Holade Y, Buchari B, Noviandri I, Kameche M, et al. Platinum nanoarrays directly grown onto a 3D-carbon felt electrode as a bifunctional material for garden compost microbial fuel cell. J Electrochem Soc 2021;168.
[39] Sanavi Fard M, Ehsani A, Soleimani F. Treatment of synthetic textile wastewater containing acid red 182 by electro-peroxone process using RSM. J Environ Manag 2023;344:118379.
[40] Flores-Rodriguez C, Reddy CNagendranatha, Min B. Enhanced methane production from acetate intermediate by bioelectrochemical anaerobic digestion at optimal applied voltages. Biomass Bioenergy 2019;127:105261.

[41] Zhang X, He W, Ren L, Stager J, Evans PJ, Logan BE. COD removal characteristics in air-cathode microbial fuel cells. Bioresour Technol 2015;176:23–31.
[42] Pei H, Yang Z, Nie C, Hou Q, Zhang L, Wang Y, et al. Using a tubular photosynthetic microbial fuel cell to treat anaerobically digested effluent from kitchen waste: mechanisms of organics and ammonium removal. Bioresour Technol 2018;256:11–6.
[43] Choi H-J, Lee S-M. Performance of Chlorella vulgaris for the removal of ammonia-nitrogen from wastewater. Environ Eng Res 2013;18:235–9.
[44] Liu Y, Qin M, Luo S, He Z, Qiao R. Understanding ammonium transport in bioelectrochemical systems towards its recovery. Sci Rep 2016;6.
[45] Salbitani G, Carfagna S. Ammonium utilization in microalgae: a sustainable method for wastewater treatment. : Sustain 2021.
[46] Wu Y-H, Yu Y, Hu H-Y, Zhuang L-L. Effects of cultivation conditions on the production of soluble algal products (SAPs) of Scenedesmus sp. LX1. Algal Res 2016;16:376–82.
[47] Jiang R, Qin L, Feng S, Huang D, Wang Z, Zhu S. The joint effect of ammonium and pH on the growth of Chlorella vulgaris and ammonium removal in artificial liquid digestate. Bioresour Technol 2021;325:124690.
[48] Singh D, Nedbal L, Ebenhöh O. Modelling phosphorus uptake in microalgae. Biochem Soc Trans 2018;46:483–90.
[49] Cai T, Park SY, Li Y. Nutrient recovery from wastewater streams by microalgae: status and prospects. Renew Sustain Energy Rev 2013;19:360–9.
[50] Sanz-Luque E, Chamizo-Ampudia A, Llamas A, Galvan A, Fernandez E. Understanding nitrate assimilation and its regulation in microalgae. Front Plant Sci 2015;6:163887.
[51] Elmaadawy K, Hu J, Guo S, Hou H, Xu J, Wang D, et al. Enhanced treatment of landfill leachate with cathodic algal biofilm and oxygen-consuming unit in a hybrid microbial fuel cell system. Bioresour Technol 2020;310:123420.
[52] Whitton R, Ometto F, Pidou M, Jarvis P, Villa R, Jefferson B. Microalgae for municipal wastewater nutrient remediation: mechanisms, reactors and outlook for tertiary treatment. Environ Technol Rev 2015;4:133–48.
[53] Esmaeili A, Moghadam HA, Golzary A. Application of marine microalgae in biodesalination and CO_2 biofixation: a review. Desalination 2023;567:116958.
[54] Zhao L, Zeng G, Gu Y, Tang Z, Wang G, Tang T, et al. Nature inspired fractal tree-like photobioreactor via 3D printing for CO_2 capture by microaglae. Chem Eng Sci 2019;193:6–14.
[55] Synodis M, Pikul J, Ann Bidstrup Allen S, Allen MG. Vertically integrated high voltage Zn-Air batteries enabled by stacked multilayer electrodeposition. J Power Sources 2020;449:227566.
[56] Elmaadawy K, Liu B, Hassan GK, Wang X, Wang Q, Hu J, et al. Microalgae-assisted fixed-film activated sludge MFC for landfill leachate treatment and energy recovery. Process Saf Environ Prot 2022;160:221–31.
[57] Walter XA, Madrid E, Gajda I, Greenman J, Ieropoulos I. Microbial fuel cell scale-up options: Performance evaluation of membrane (c-MFC) and membrane-less (s-MFC) systems under different feeding regimes. J Power Sources 2022;520:230875.
[58] Sanavi Fard M, Ehsani A, Soleimani F. Optimization of Toluenediamine degradation in synthetic wastewater by a UV/H2O2 process using full factorial design. Water Resour Ind 2023;30:100218.